Supplementary Information

S1.1 Stereological calculations:

Step 1: Calculating total *f*MWCNT length within the intracellular and basolateral BBB compartments of the TEM sections

To calculate *f*MWCNT length, we used the approach of Cruz-Orive and Howard (methods described in detail in reference 1) proposing that the total length of the space (3D) curve can be estimated from its 2D "vertical" projection. A cycloid grid (fig. S1) was selected for the stereological calculations to ensure that the *f*MWCNT intersection count was isotropic, *i.e.* that no orientation in three dimensions was favoured.

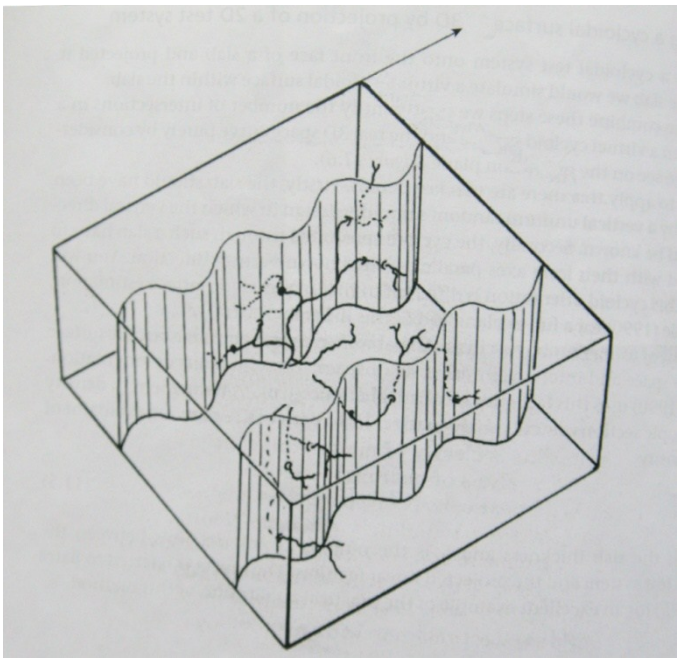

Figure S1. The total vertical projections method for estimation of total length of linear features. A set of cycloids is projected through the recording slab to generate a set of virtual cycloid surfaces. The number of intersections between these virtual surfaces and the linear features gives an unbiased estimate of their length. Modified from Howard *et al*[1].

The total length L_c of the *f*MWCNT in the TEM imaged volume is estimated from

$$L_c = 2\, I \times A/L \qquad (1)$$

Where I is the number of *f*MWCNT intersections with cycloids, and A/L is the reciprocal of the length of the cycloid per unit area (defined as the area of cycloid grid divided by 2×cycloid radius). A/L = 197 nm for the cycloid grid employed here.

The total length of the *f*MWCNT within the cell and basal compartments (between the cells and the transwells) was calculated from equation (1) employing the respective cycloid crossing count for each compartment.

Step 2: Scaling up measured *f*MWCNT length in the imaged TEM to total *f*MWCNT length per transwell

To scale up the length of *f*MWCNT imaged in the TEM sections to the total *f*MWCNT length within each transwell the following scaling factor was applied,

$$S = A/B \tag{2}$$

where, A is the total area of the transwell filter (radius = 6mm in our setup) and B is the transwell area covered by the TEM images, given by

$$B = (L_t)\,(D) \tag{3}$$

where L_t is the total length of the transwell observed, as measured from the total length of the TEM image montages (200 to 300 μm in our experiments) (fig. S2), and D is the microtomed section thickness (100 nm in our experimental setup).

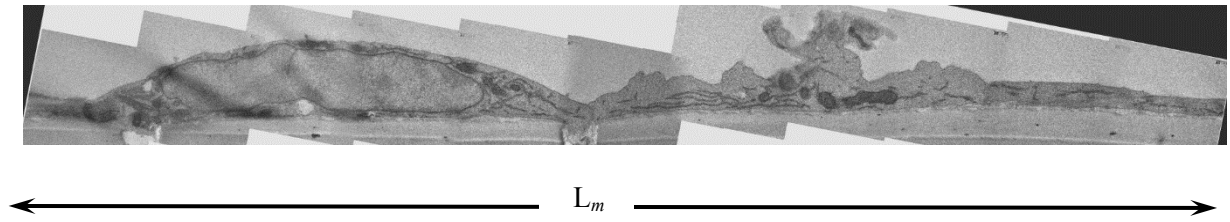

Figure S2. Example of a TEM montage from hCMEC/D3 cells exposed to the PEG-MWCNT used to calculate the total transwell length imaged. The length of every montage (L_m) employed to image the TEM zone was summed to calculate the total imaged length (Lt).

Step 3: Conversion from *f*MWCNT length to *f*MWCNT mass

The carbon mass per unit length of *f*MWCNT was calculated from the number of CNT walls constituting the *f*MWCNT. Wall number was estimated from the difference between the inner and outer diameter measured through TEM (Fig. S3), equating to an average of 9.8 nm estimated from measurement of at least 150 individual MWCNTs (see section S1.2 below). Assuming an interplanar distance of 0.34 nm as per the structure of 3D crystalline graphite[2,3], the diameter difference equates to a wall number of 14.

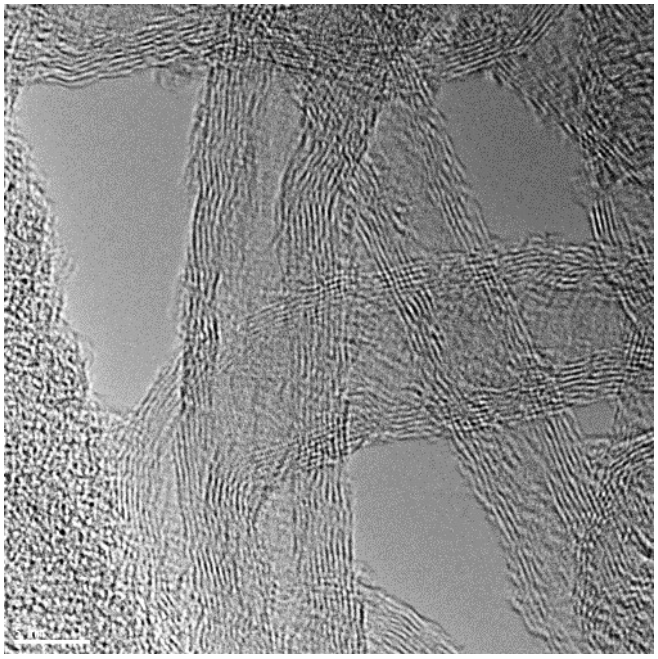

Figure S3. An example of a TEM image of a *f*MWCNT employed to calculate the number of walls per carbon nanotube as an estimate of the difference between the inner and outer CNT diameter (scale bar = 5 nm).

The area per carbon atom occupied in each CNT wall was calculated from the hexagonal carbon atom arrangement of each 'building unit' of the *f*MWCNT (fig. S4).

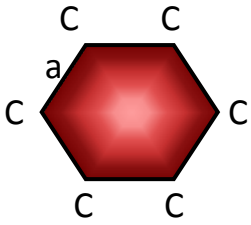

Figure S4. The schematic structure of a MWCNT used in this study, displaying the hexagonal arrangement of each carbon atom within the CNT wall. The carbon-carbon length 'a' was employed to calculate the hexagonal area, from which the area occupied by each carbon was calculated.

In the hexagonal arrangement, the C-C bond 'a' occupies length = 0.142 nm.

The *f*MWCNT mass (in grams) in each localization was thus calculated from *f*MWCNT length using the following equations:

Hexagonal area:

$$A = \frac{3\sqrt{3}}{2}a^2 \tag{4}$$

Area per carbon atom:

$$\frac{1}{2} \times \frac{3\sqrt{3}}{2} \times (0.142\ nm)^2 = 0.0262\ nm^2 \tag{5}$$

(The factor of ½ arises since there are 6 carbon atoms in the hexagon and each carbon atom has 3 nearest neighbours).

The number of carbon atoms per unit length was subsequently calculated from the total CNT surface area per unit length as per the below table:

wall#	Radius, r (nm)	circumference (nm)	CNT length, l (nm)	area (nm^2)	# C atoms/unit length of MWCNT
n	$r_{n+1} - 0.34$	$2\pi r_n$	1	$2\pi r_n * l$	$2\pi r_n \div 0.0262$
1	6.1 ± 0.145	38.33 ± 0.91	1	38.33 ± 0.91	1462.88 ± 34.7
2	5.76 ± 0.145	36.19 ± 0.91	1	36.19 ± 0.91	1381.34 ± 34.7
3	5.42 ± 0.145	34.06 ± 0.91	1	34.06 ± 0.91	1299.80 ± 34.7
4	5.08 ± 0.145	31.92 ± 0.91	1	31.92 ± 0.91	1218.27 ± 34.7
5	4.74 ± 0.145	29.78 ± 0.91	1	29.78 ± 0.91	1136.73 ± 34.7
6	4.4 ± 0.145	27.65 ± 0.91	1	27.65 ± 0.91	1055.19 ± 34.7
7	4.06 ± 0.145	25.51 ± 0.91	1	25.51 ± 0.91	973.65 ± 34.7
8	3.72 ± 0.145	23.37 ± 0.91	1	23.37 ± 0.91	892.12 ± 34.7
9	3.38 ± 0.145	21.24 ± 0.91	1	21.24 ± 0.91	810.58 ± 34.7
10	3.04 ± 0.145	19.10 ± 0.91	1	19.10 ± 0.91	729.04 ± 34.7
11	2.7 ± 0.145	16.97 ± 0.91	1	16.97 ± 0.91	647.50 ± 34.7
12	2.36 ± 0.145	14.83 ± 0.91	1	14.83 ± 0.91	565.97 ± 34.7
13	2.02 ± 0.145	12.69 ± 0.91	1	12.69 ± 0.91	484.43 ± 34.7
14	1.68 ± 0.145	10.56 ± 0.91	1	10.56 ± 0.91	402.89 ± 34.7

Total number of carbon atoms per unit length of *f*MWCNT = 13060.4 ± 486/nm

Total mass of CNTs per unit length is given by

$$\text{CNT mass} = (13060.4)\ (M_C)\ (N_A)^{-1} \tag{6}$$

where M_C = 12 g/mol (molecular weight of carbon) and Na is Avogadro's number, giving $2.603 \times 10^{-19} \pm 0.097 \times 10^{-19}$ g/nm

To convert total CNT length to CNT mass in each compartment equation 7 is applied

$$\text{Total MWCNT mass (g) in each compartment} = L_c \times 2.603 \times 10^{-19} \times S \tag{7}$$

Where S is the scaling factor in equation (2) and L_c is the quantified CNT length from equation (1).

Step 4: Measurement of % ID

The %ID (initial dose) was calculated by dividing the mass of *f*MWCNT in each BBB compartment by the ID applied to the cells.

Sources of errors:

The accuracy of the measurement of total *f*MWCNT in each transwell from the stereological calculations is sensitive to changes in section volume due to microtoming/embedding/imaging artefacts, including compression and shrinkage. As the cutting direction is in the plane of the transwell, compression artefacts will dominate the error: the percentage area of the transwell is underestimated, so the %ID will be slightly overestimated. However, the ratio of % ID in the intracellular:basal compartments measured by TEM will not be affected by this error as we can assume the compression artefact does not vary between the compartments.

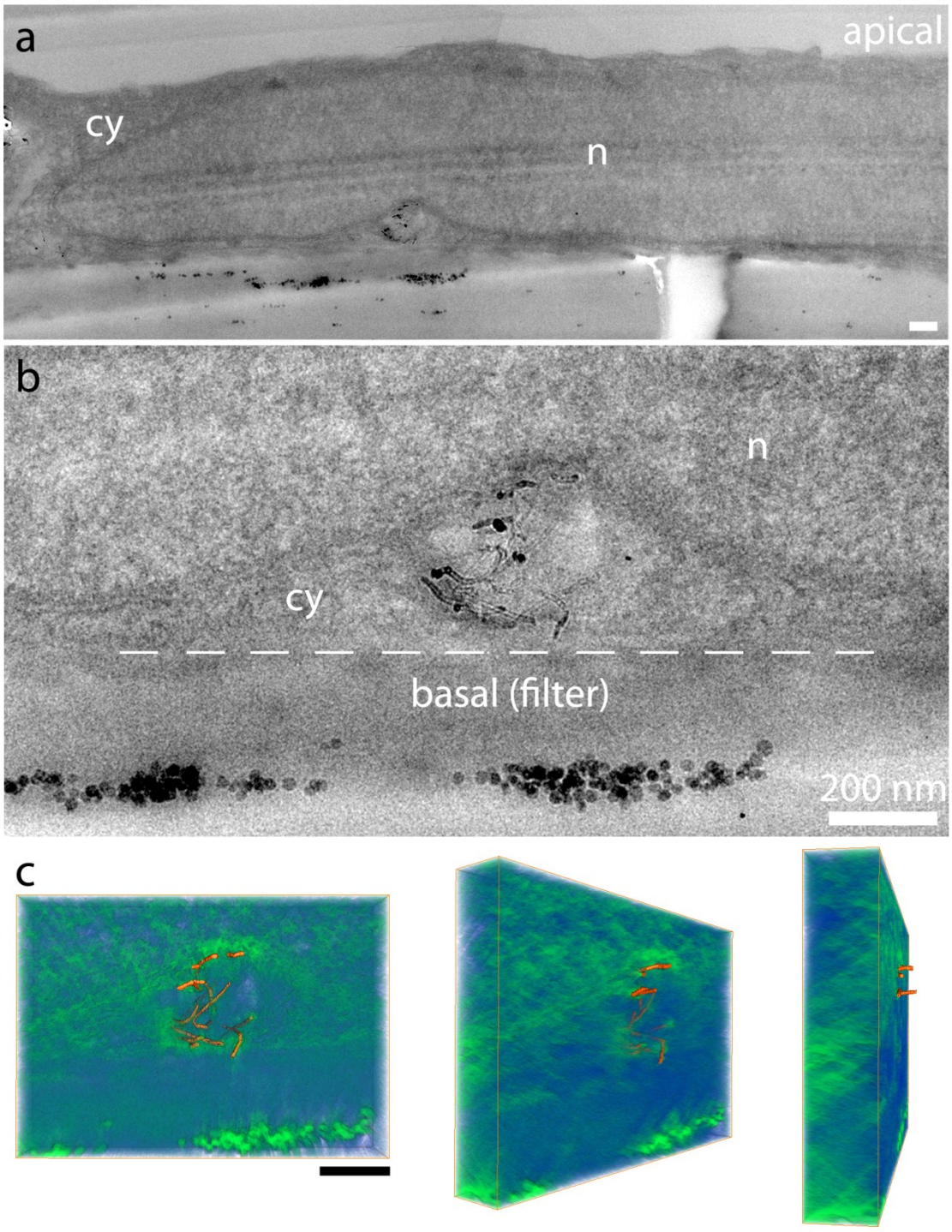

Figure S4. TEM tomography reconstruction showing the location of M4VP-MWCNT within an embedded cell section. Bright field TEM images at low (a) and higher (b) magnification of a cluster of MWCNT at the basolateral side of an hCMEC/D3 cell, and (c) tomographic reconstruction of the same vesicle viewed from various angles, showing that the majority of CNT are located within the embedded section. The cell nucleus (n), cytoplasm (cy) are labelled, and the boundary between the cell and basolateral filter membrane is indicated by the dashed line in (b) for clarity. All scale bars = 200nm.

1.2 TEM measurement of MWCNT inner and outer diameter. MWCNT powders were dispersed in 10 ml deionised water with 10 minute bath sonication (VWR Ultrasonic Cleaner, 80W) followed by 2 minute probe sonication at 30% power (Sonics Vibra Cell™, 750W). Solutions were then drop cast onto lacey carbon coated copper TEM grids (TAAB, 400 mesh, 3 mm copper grid) supported by filter paper. Bright field (BF) and high resolution phase contrast imaging was carried on an FEI Titan 80-300 scanning/transmission electron microscope (S/TEM) operated at 80kV. Bright-field TEM (BF-TEM), and high-resolution TEM (HRTEM) images were captured on a Gatan 2kx2k CCD camera US1000. The accelerating voltage used in this study was 80kV which is below the critical threshold energy predicted for severe knock-on damage in CNTs [42]. In order to confirm that no damage to the MWNTs had occurred under the electron beam time course beam damage studies were undertaken. In HRTEM images, no visible damage to the MWNTs was observed after direct exposure to the beam for 60 min. The inner and outer diameters of at least 150 individual MWCNTs, sampled from five different areas of the TEM grid, were measured for each sample, to provide a statistically accurate representation of diameter distributions. Measurements carried out using ImageJ.

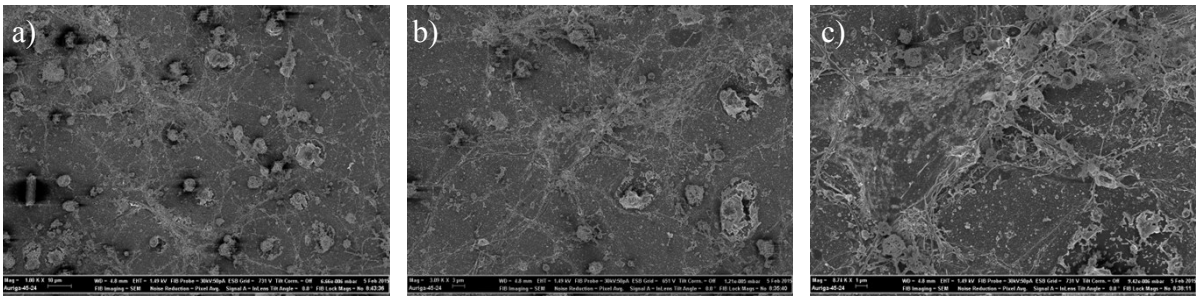

Figure S5. SEM images of untreated primary hippocampal neurons at low (a), middle (b) and high (c) magnification.

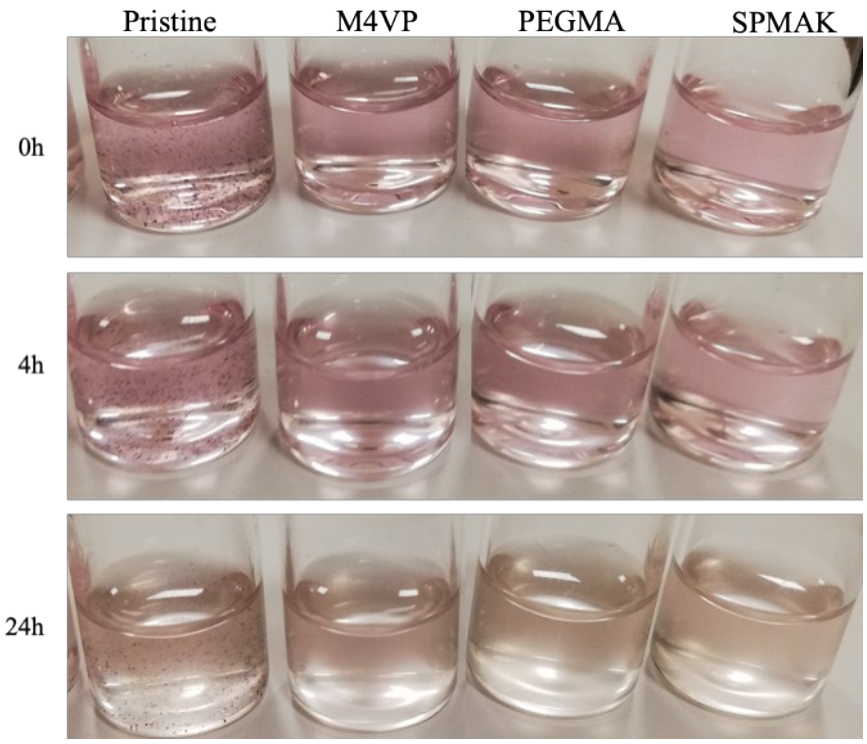

Figure S6. Examination of fMW-CNT aggregation in cell culture medium containing 2.5% FBS. Carbon nanotubes were incubated in cell culture medium containing 2.5% FBS for 0h, 4h and 24h. CNT were then visualized to examine precipitation as a marker of aggregation. Sedimentation of functionalized (f)MW-CNT was compared to that of pristine (unfunctionalized) MW-CNT.

Table 2. *Z-average and PDI of functionalized CNT at 0h, 4h and 24h incubation in 2.5% FBS cell culture media (measurements for cell culture media without CNTs is also displayed)*

Sample	**0h**		**4h**		**24h**	
	Z-average (nm)	**PDI**	**Z-average (nm)**	**PDI**	**Z-average (nm)**	**PDI**
Cell Media	209.5	0.43	217.6	0.38	210.8	0.36
M4VP	284.7	0.43	293.9	0.43	308.2	0.52
PEGMA	258.2	0.33	227.9	0.31	237.8	0.36
SPMAK	315.9	0.48	265.6	0.47	277.2	0.43

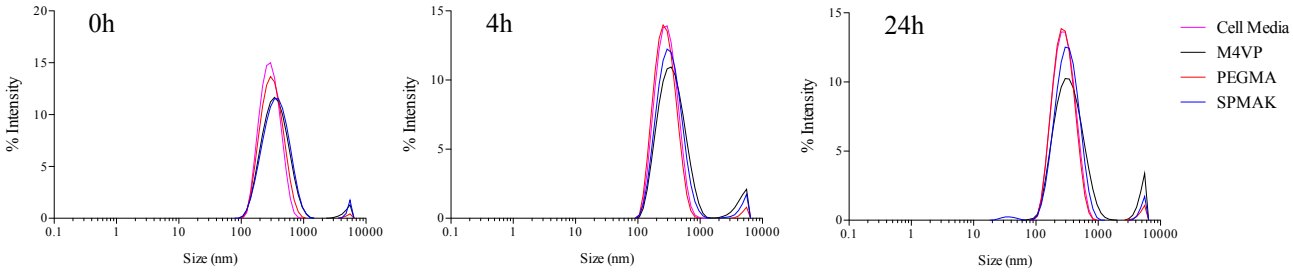

Figure S7. *DLS histograms of functionalized MWCNT at 0h, 4h and 24h incubation time in cell culture media with 2.5% FBS (histograms for cell culture media without CNTs is also displayed).*

Reference:

[1]Howard CV and Reed MG (1993). Unbiased Stereology. Second Edition. 2:113-120, BIOS Scientific Publishers. Taylor & Francis Group.

[2]Endo M, T Hayashi, and Kim Y. Large-scale production of carbon nanotubes and their applications. Pure and applied chemistry, 2006. 78 (9): p. 1703-1713.

[3]Firme C, Bandaru P. Toxicity issues in the application of carbon nanotubes to biological systems. Nanomedicine, 6 (2): 245-56, 2010.